PHYSICAL REVIEW A VOLUME 50, NUMBER 4 OCTOBER 1994

Inelastic electron–dipole-molecule scattering at sub-milli-electron-volt energies: Possible role of dipole-supported states

M. T. Frey, S. B. Hill, X. Ling, K. A. Smith, and F. B. Dunning
Department of Physics and the Rice Quantum Institute, Rice University, P.O. Box 1892, Houston, Texas 77251

I. I. Fabrikant
Department of Physics and Astronomy, University of Nebraska, Lincoln, Nebraska 68588

(Received 20 April 1994)

Studies of collisions between Rydberg atoms with values of principal quantum number n in the range $100 \lesssim n \lesssim 400$ and H_2S and $C_6H_5NO_2$ are reported. These targets were selected because they have very different dipole moments: 0.97 and 4.22 D, respectively. Analysis of the data using the essentially-free-electron model shows that at micro-electron-volt energies the cross sections for rotationally inelastic electron scattering by these targets have very different energy dependences. This difference suggests that, in the case of $C_6H_5NO_2$, dipole-supported states might be important in the scattering. To examine this further, the data are compared with the results of calculations using a free-electron cross section that assumes the presence of dipole-supported states, and it is demonstrated that, with a reasonable choice of parameters, it is possible to reproduce the experimental observations.

PACS number(s): 34.80.−i

For sufficiently large values of principal quantum number n, collisions involving Rydberg atoms can be described using the essentially-free-electron model, originally proposed by Fermi, which assumes that the separation between the excited Rydberg electron and its associated core ion is so large that both do not interact simultaneously with a target particle [1]. Thus, because the time average kinetic energy of the Rydberg electron ($\sim 13.6/n^2$ eV) is very small, studies of Rydberg atom collision processes that are dominated by the binary Rydberg electron–target interaction can provide information on electron–molecule scattering. This approach has been used to study electron capture and electron–polar-molecule scattering at micro-electron-volt energies [2,3]. In collisions with polar targets, transfer of molecular rotational energy to the Rydberg electron through superelastic scattering in a binary electron–target interaction can lead to near-resonant excitation to higher-lying states or, if the energy transfer is sufficient, to ionization [4-6]. Rate constants for destruction, i.e., ionization, of potassium Rydberg atoms through rotational energy transfer in collisions with HF, NH_3, CH_3I, and CH_2Br_2 have been previously measured for values of n in the range $100 \lesssim n \lesssim 400$ [3]. The data reveal a marked n dependence that is inconsistent with free-electron scattering cross sections derived using the Born approximation [7]. One possible explanation suggested for this discrepancy is that dipole-supported states might be important in the scattering. To examine this possibility further, we have extended studies of Rydberg atom–polar-molecule collisions to include targets with a broader range of dipole moments, specifically H_2S (0.97 D) and $C_6H_5NO_2$ (4.22 D). (The dipole moments for targets studied previously all lie in the range 1.43–1.82 D.) Although the behavior observed with $C_6H_5NO_2$ is similar to that observed earlier with other targets, that for H_2S is quite different. No strong n dependence in the measured destruction rate constants is apparent, and the data suggest that the free-electron cross section scales as $1/v$, where v is the electron velocity, which is consistent with the Wigner threshold law for an s-wave process [8]. Because of its small dipole moment, it is unlikely that dipole-supported states will be important in scattering from H_2S, indicating that the quite different behavior observed with the other polar targets might indeed be associated with such states. To examine this further, the n dependence of the rate constants for Rydberg atom destruction was calculated using a free-electron-scattering cross section that assumes the presence of dipole-supported states. These calculations demonstrate that, with a reasonable choice of parameters, it is possible to reproduce the n dependence observed earlier.

The apparatus and techniques used in the present investigation are described in detail elsewhere [2,3]. Pulses of potassium atoms in selected high-lying np states are created, in zero electric field and in the presence of target gas, by laser-induced photoexcitation. Rate constants for the different collisional processes of interest are determined by measuring the subsequent time evolution of the Rydberg atom population in the experimental volume using selective field ionization (SFI). In SFI a ramped electric field is applied in the experimental volume. Because Rydberg atoms in different excited states ionize at different applied fields, measurement of the field ionization signal as a function of the applied field provides a measure of the distribution of excited states in the experimental volume immediately prior to application of the field. Quasielastic scattering of the Rydberg electron by a target molecule can lead to so-called l-changing reactions that populate states having a small range of n close to the initial value but a near-statistical mix of l. Inelastic scattering can lead to near-resonant rotational energy

1050-2947/94/50(4)/3124(5)/$06.00

transfer resulting in so-called n-changing reactions that populate localized groups of higher n states, or, if the energy transfer is sufficient, in ionization.

In the case of H_2S, SFI measurements showed that for the present range of n the rates for l changing and n changing were very small. Collisional destruction of Rydberg atoms in the experimental volume is therefore associated primarily with collisional ionization of parent np atoms through rotational energy-transfer reactions of the type

$$K(np)+H_2S(J,\tau)\rightarrow K^+ + H_2S(J',\tau')+e^- \ . \qquad (1)$$

The measured rate constants for collisional destruction through this reaction are shown in Fig. 1(a). In contrast, for $C_6H_5NO_2$, SFI measurements showed that the parent np states undergo rapid l mixing (at $n=150$ the measured rate constant for l changing was $\sim 1\times 10^{-5}$ $cm^3\,sec^{-1}$) and the excited-state distribution in the experimental volume quickly evolves into a near-statistical mix of l states with values of n close to that of the parent np states. As discussed elsewhere, the products of such l-changing reactions can be viewed as a single "mixed" reservoir whose population distribution is unaffected by subsequent l-changing reactions [4,6]. Atoms can, however, be removed from this reservoir by n-changing and collisional ionization reactions of the type

$$K(nl)+C_6H_5HO_2(J,\tau)\rightarrow\begin{cases}K(n'l')+C_6H_5NO_2(J',\tau') & (2a)\\ K^+ + C_6H_5NO_2(J',\tau')+e^- \ . & (2b)\end{cases}$$

(At room temperature a significant fraction of the target molecules are in vibrationally excited states, and rotational energy transfer may be accompanied by transfer of vibrational energy.) $C_6H_5NO_2$, however, also attaches free low-energy electrons and the l-mixed reservoir can be depleted through electron transfer reactions of the type

$$K(nl)+C_6H_5NO_2\rightarrow K^+ + C_6H_5NO_2{}^- \ , \qquad (3)$$

in which the excited Rydberg electron is captured by the target. Long-lived ($\tau \gtrsim 50$ μsec) $C_6H_5NO_2{}^-$ ions were detected but ancillary measurements showed that the rate constants associated with reaction (3) are small, $\sim 5\times 10^{-8}$ $cm^3\,sec^{-1}$. This process therefore does not contribute significantly to reservoir depletion and is neglected. (No long-lived H_2S^- ions were observed following Rydberg atom collisions with H_2S suggesting that negative ion formation is not an important channel for Rydberg atom destruction in collisions with H_2S.) Measured rate constants for depletion of the l-mixed reservoir through the combination of reactions (2a) and (2b) are presented in Fig. 1(b).

Figure 2 shows a comparison between the present results and representative data obtained previously with other targets [3], for which Rydberg atom destruction also results primarily from rotational energy transfer. For the range of n encompassed in Fig. 2, rotational energy transfer in collisions with HF and NH_3 leads directly to ionization. In the case of CH_2Br_2, the large majority of the possible rotational transitions results in ionization. The data for HF refer to destruction of atoms in the parent np state, whereas the data for NH_3 and CH_2Br_2 are for an l-mixed population. The rate constants measured with $C_6H_5NO_2$ and H_2S clearly bound those observed earlier with targets having "intermediate" dipole moments.

Assuming that Rydberg atom destruction (and reser-

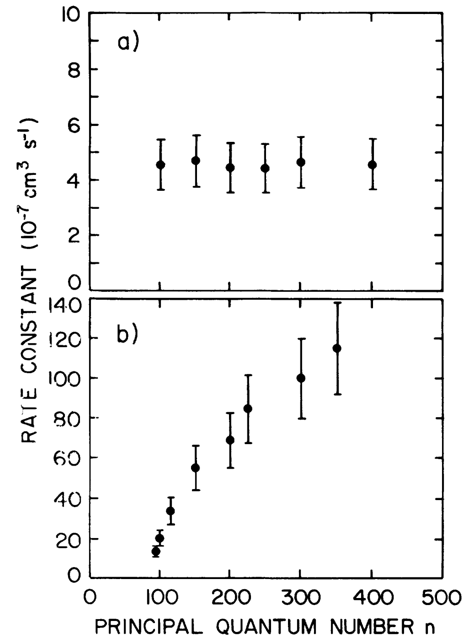

FIG. 1. (a) Rate constants for destruction of K(np) atoms in collisions with H_2S. (b) Rate constants for destruction of an l-mixed population (see text) in collisions with $C_6H_5NO_2$.

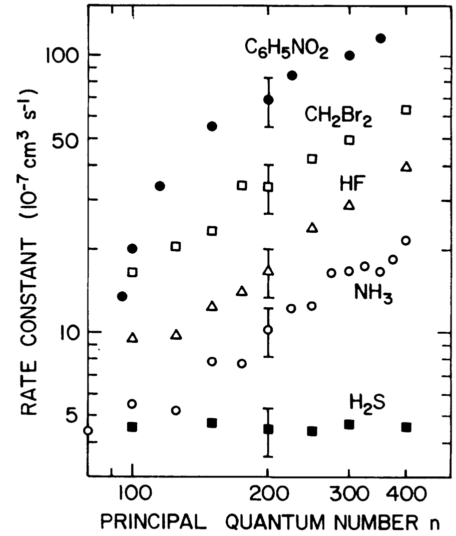

FIG. 2. Comparison of rate constants for Rydberg atom destruction in collisions with several different targets. The data for H_2S and HF are for destruction of parent K(np) atoms, the data for NH_3, CH_2Br_2 and $C_6H_5NO_2$ are for an l-mixed population.

voir depletion) is associated with rotationally inelastic scattering of the Rydberg electron, the essentially-free-electron model requires that the rate constant for collisional destruction (depletion) should equal that for rotational deexcitation of the target by free electrons having the same velocity distribution as the Rydberg electrons, i.e.,

$$k=\int_0^\infty v\sigma_e(v)f(v)dv \ , \tag{4}$$

where $\sigma_e(v)$ is the cross section for rotationally inelastic scattering of free electrons with velocity v, and $f(v)$ is the Rydberg electron velocity distribution, which depends on the particular excited state, or excited-state distribution, considered. The rate constants measured for H_2S are independent of n, i.e., independent of $f(v)$. Inspection of Eq. (4) shows that such behavior requires that the cross section $\sigma_e(v)$ vary as $1/v$, which is consistent with the Wigner threshold law for an s-wave process [8]. This is, at first sight, perhaps surprising because the Wigner threshold law is not expected to be valid for scattering from a $1/r^2$ dipole potential [9]. In the present case, however, the energy of the incident electrons is low. The electron-target interaction lasts so long that molecular rotation becomes important, and the interaction cannot be viewed simply as scattering from a static $1/r^2$ potential [10]. Rather, the electron experiences a potential that represents some average over molecular orientation. H_2S is an asymmetric top ($A=10.374$ cm^{-1}, $B=8.991$ cm^{-1}, and $C=4.732$ cm^{-1}) and thus, over sufficiently long times, the target dipole moment will average to zero as observed in a laboratory-fixed frame. This does not mean that there is no interaction between the electron and target molecule, however, because, in essence, the electron induces a net dipole moment in the target. Since the resulting interaction potential decreases faster than $1/r^2$, it is not unreasonable to expect that the Wigner $1/v$ threshold law might apply. [At higher electron energies it is reasonable to adopt a fixed-nucleus, static-dipole approximation under which conditions the cross section $\sigma_e(v)$ for all rotational transitions should scale as $1/v^2$ [11]].

The near-linear increase with n in the measured rate constants for depletion of the l-mixed reservoir through collisions with $C_6H_5NO_2$ for $n \gtrsim 200$ contrasts the behavior observed with H_2S. As evident from Fig. 2, however, such behavior is similar to that noted earlier using simpler targets, although the rate constants for $C_6H_5NO_2$ are significantly larger, presumably reflecting its greater dipole moment. Clearly, the observed increase with n is inconsistent with the simple Wigner threshold law for an s-wave process. Indeed, the data are consistent with a scattering cross section $\sigma_e(v)$ that scales as $1/v^2$, i.e., as the square of the electron de Broglie wavelength. (In this event, k scales as $\langle 1/v \rangle$, which is approximately proportional to n.) As n decreases below ~ 200, n changing [reaction 2(a)] becomes increasingly important relative to collisional ionization [reaction 2(b)] in depleting the l-mixed reservoir. At $n=200$, almost all possible rotational transitions in $C_6H_5NO_2$ lead to ionization, but this decreases to approximately one-half at $n \sim 150$ and to a few percent at $n \sim 100$. Thus, since rotational energy transfer requires near energy resonance, the pronounced decrease in the measured rate constants observed below $n \sim 150$ may result because as n becomes smaller the density of final states that can be populated through a particular rotational transition is reduced.

H_2S has a relatively small dipole moment, suggesting that the differences between its behavior and that of the other targets studied to date might be associated with their larger dipole moments. A static dipole with dipole moment greater than the critical value $\mu_{\rm cr} \sim 1.625$ D can support an infinite number of bound states [12]. However, if rotation is included all or many of these states disappear [13]. For example, LiF, which has a relatively large dipole moment, 6.3 D, can support only two excited $^2\Sigma^+$ states with binding energies $\sim 4.9\times 10^{-3}$ and 2.3×10^{-6} eV [10]. HF has a supercritical dipole moment, 1.82 D, but this is insufficient to retain any bound states when rotation is included. Nonetheless, theory suggests that, at least for the ground rotational state, a virtual HF^- state exists with an energy in the range 10^{-4}–10^{-5} eV, although this result is tentative because *ab initio* calculations are difficult due to the very diffuse nature of dipole-supported states [10]. Since in HF the dipole moment is aligned along the internuclear axis, and rotation, which occurs about an axis perpendicular to the internuclear axis, causes the dipole moment to rapidly average to zero, this state must be associated with an electron-induced dipole interaction. Such interactions are described by the attractive polarization potential $-\alpha/2r^4$ for the ground rotational state, where α is the effective molecular polarizability, and by a dynamic polarization interaction decaying as $1/r^6$ for higher rotational states [14]. (Polarization effects associated with the core ion should be negligible because, for the present range of n, the size of the Rydberg atoms is such that the separation between the core ion and an interacting electron–target molecule pair will typically be very much greater than the range of the electron–target interaction.) In the absence of any long-range $1/r^2$ interaction due to some "nonaveraged" residual component of the dipole moment, the presence of a dipole-supported virtual state will lead to a cross section for superlastic free-electron scattering of the form [15]

$$\sigma_e(v)=\frac{a}{v(v^2+\kappa^2)} \ , \tag{5}$$

where v is the electron velocity in atomic units, a is a constant, and $-\kappa^2/2$ is the energy of the dipole-supported state. This expression, however, assumes that only the s-wave component of the initial-state wave function is important, and that all other components may be neglected. Although shape resonances may appear in higher partial waves, their relative contribution to the total cross section should be much smaller due to the Wigner threshold-law factor v^{2l-1}.

Because the dipole moment for HF rapidly averages to zero, it is reasonable to consider using the expression for $\sigma_e(v)$ given in Eq. (5) in analyzing the data. Substitution of an expression of this form in Eq. (4), together with the approximate classical velocity distribution $f(v)$ appropriate to np states [16]

$$f(v)=\frac{4n}{\pi(1+n^2v^2)^2}\ , \tag{6}$$

(collisions with HF do no lead to rapid l-changing) yields a relatively simple expression for the rate constant k,

$$k=a(n|\kappa|+2)\frac{n}{|\kappa|(n|\kappa|+1)^2}\ , \tag{7}$$

The n dependence of the rate constants k predicted by Eq. (7) is shown in Fig. 3 for values of $|\kappa|$ of 3×10^{-4}, 1×10^{-3}, and 3×10^{-3} a.u. It is evident from Fig. 3 that with an appropriate choice of $|\kappa|$ the general features of the HF experimental data, namely, an approximately linear increase in k with n (over the range $100\lesssim n\lesssim400$) and a near-zero intercept with the k axis, can be reproduced. The observed behavior is consistent with that predicted by Eq. (7) provided that $|\kappa|$ is less than $\sim1\times10^{-3}$ a.u. This corresponds to virtual state energies below $\sim1.4\times10^{-5}$ eV which, as might be expected, are small. The experimental data, however, pertain to target molecules with a thermal (300 K) rotational population distribution. It is quite possible that the energies of the dipole-supported states important in the scattering could depend on the rotational state of the target. (The binding energy of the bound states decreases as the rotational quantum number increases [17]). Thus any values of $|\kappa|$ derived by comparing the experimental data with the theoretical expressions must represent some average over the target rotational distribution.

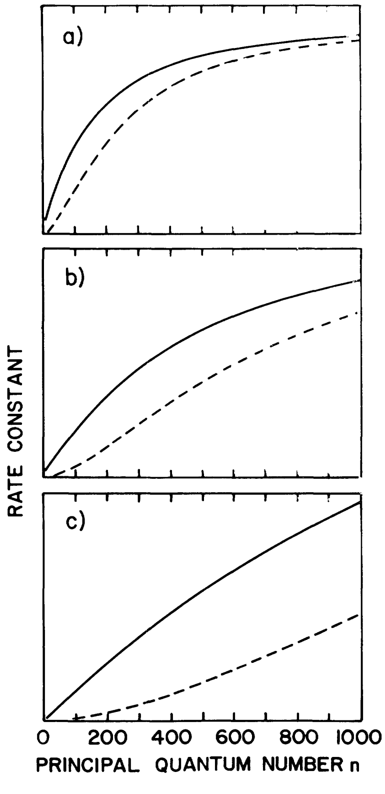

FIG. 3. Calculated n dependence of the rate constants for destruction of Rydberg atoms in the parent np state (——) and in an l-mixed reservoir (— — —). These were derived using the expression for $\sigma_e(v)$ given in Eq. (5) assuming values of $|\kappa|$ of (a) 3×10^{-3}, (b) 1×10^{-3}, and (c) 3×10^{-4} a.u.

Application of the expression given in Eq. (5) to the more complex rotors discussed here must be approached with caution. $C_6H_5NO_2$ is an asymmetric top ($A=0.1323$ cm^{-1}, $B=0.0429$ cm^{-1}, and $C=0.0324$ cm^{-1}), and it is reasonable to expect that, over sufficiently long times, its dipole moment will average to zero. Rydberg atom collisions with $C_6H_5NO_2$ (and CH_2Br_2 and NH_3), however, lead to rapid l mixing. For a collection of atoms with the same value of n but a statistical distribution of l values, the overall electron velocity distribution function is given approximately by [18]

$$f(v)=\frac{32}{\pi}\frac{n^3v^2}{(n^2v^2+1)^4}\ . \tag{8}$$

Use of this expression in Eq. (4), together with $\sigma_e(v)$ given by Eq. (5), predicts a rate constant k of the form

$$k=a(n^2\kappa^2+4n|\kappa|+5)\frac{n^2}{(n|\kappa|+1)^4}\ . \tag{9}$$

Values of k derived using Eq. (9) are included in Fig. 3. Although k initially increases quadratically with n for small values of $n|\kappa|$, a linear dependence is again evident for intermediate values of $n|\kappa|$. However, it should be noted that both Eqs. (7) and (9) predict that for values of n such that $n|\kappa|$ is large, k will become independent of n consistent with the Wigner $1/v$ threshold law for an s-wave process. The n dependence of the experimental data (at high n) is consistent with that suggested by Eq. (9) for values of $|\kappa|\sim1\times10^{-3}$ a.u. which correspond to a virtual (or bound) state energy of $\sim1.4\times10^{-5}$ eV.

CH_2Br_2 approximates a prolate symmetric top ($A=0.868$ cm^{-1}, $B=0.041$ cm^{-1}, and $C=0.039$ cm^{-1}). For such targets the dipole moment will not average to zero if K, the projection of the angular momentum along the axis, is not equal to zero and if the component of the dipole moment along this axis is nonzero. However, for a room-temperature thermal distribution, the rotational states with the largest populations correspond to large values of J and small K. Thus any "nonaveraged" component of the dipole moment should be small. (A similar argument can also be applied in the case of $C_6H_5NO_2$ if it is approximated as a prolate symmetric top.) NH_3, however, is an oblate symmetric top ($B=9.444$ cm^{-1} and $C=6.196$ cm^{-1}) and at room temperature states of large K (relative to J) tend to dominate the distribution. (One more complication in NH_3 is its large inversion splitting, 0.8 cm^{-1}, which splits the $\pm K$ pairs into parity eigenstates and restores the Wigner law [19].) In the presence of a "nonaveraged" component of the dipole moment the interaction potential contains both a long-range $1/r^2$ component and a shorter-range contribution due to polarization interactions. This "composite" potential may again support bound or virtual states, and bound states may exist even if the reduced "nonaveraged" dipole moment is subcritical. The existence of a dipole-supported state together with a "nonaveraged" reduced dipole moment leads to the following expression for the cross section for superelastic free-electron scattering [20]:

$$\sigma_e(v)=\frac{a}{v^2}\left|\frac{v^{\lambda+1/2}}{\eta-ie^{-i\pi\lambda}v^{2\lambda+1}}\right|^2 , \qquad (10)$$

where η is a constant and λ is a parameter that depends on the angular momentum quantum numbers and the reduced dipole moment, which can be obtained by diagonalizing the strong-coupling matrix introduced by Engelking [21]. The parameter η is simply related to the energy of the dipole-supported state [11]. If the reduced dipole moment is subcritical, λ is real, and $\eta=-\kappa^{2\lambda+1}$, where $-\kappa^2/2$ is, as before, the energy of the virtual (for $\eta>0$) or bound (for $\eta<0$) state. Note that, if the reduced dipole moment is small, λ is close to the orbital angular momentum of the incident electron, i.e., $\lambda\approx 0$ for s-wave scattering, and we recover Eq. (5). If the reduced dipole moment is appreciable the deviation of the threshold exponent $x=2\lambda+1$ from 1 may be substantial. For example, at room temperature the most highly populated NH_3 rotational state corresponds to $J=3$, $K=3$, followed by $J=4$, $K=3$. The corresponding threshold exponents are $x=0.606$ and 0.782, respectively. The n dependences observed with NH_3 and CH_2Br_2 are again consistent with scattering involving dipole-supported states with energies of $\sim 10^{-4}-10^{-5}$ eV.

The present work shows that the n-dependence in the measured rate constants for Rydberg atom destruction through rotational energy transfer in collision with polar targets is in accord with a free-electron-scattering cross section that takes into account dipole-supported virtual (or bound) states. (Such states do not appear to be important, however, in scattering from H_2S, presumably because its polarizability is small.) This suggests that dipole-supported states might be important in electron–polar-molecule scattering at ultralow electron energies. However, the data in Figs. 1 and 2, which span the range $100\lesssim n\lesssim 400$, do not clearly demonstrate that the free-electron cross sections given in Eqs. (5) and (10) are to be preferred over simpler forms such as a $1/v^2$ dependence which, as noted previously, also predicts a near-linear increase in k with n. Better discrimination between different possible forms of the cross section can be obtained by extending measurements to larger values of n, say $n\gtrsim 1000$. (It must be remembered, however, that for values of $n\gtrsim 1000$ the "orbital" velocity of the Rydberg electron is sufficiently low that the relative Rydberg atom–target molecule motion becomes significant and perturbs the Rydberg electron velocity distribution as observed in the rest frame of the target molecule.) For example, the rate constants k predicted using the free-electron cross section given in Eq. (5) tend to a constant value for large values of n (see Fig. 3), whereas the rate constants derived assuming a $1/v^2$ dependence continue to increase almost linearly. Fits to measurements spanning a broader range of n would also provide tighter bounds on the inferred values of $|\kappa|$. Further information as to the appropriate form of the free-electron cross section may be obtained by comparing measurements of collisional depopulation made at the same value of n with parent np states and with an l-mixed population. (Such measurements will, however, be difficult because polar targets frequently have very large rate constants for l changing.) As evident from Fig. 3, calculations show that the ratio of the rate constants for collisional depopulation of parent and mixed states is quite sensitive to the assumed form of the free-electron cross section, and to the value of $|\kappa|$. Clearly, however, Rydberg atoms provide a tool with which to examine threshold behavior in electron–dipole-molecule scattering.

This research is supported by the National Science Foundation under Grant Nos. PHY-9113414 and PHY-9207986, and the Robert A. Welch Foundation.

---

[1] E. Fermi, Nuovo Cimento **11**, 157 (1934). For a more detailed discussion of the essentially-free-electron model, see, for example, the articles by M. Matsuzawa and by A. P. Hickman, R. E. Olson, and J. Pascale in *Rydberg States of Atoms and Molecules,* edited by R. F. Stebbings and F. B. Dunning (Cambridge University Press, New York, 1983).
[2] X. Ling, B. G. Lindsay, K. A. Smith, and F. B. Dunning, Phys. Rev. A **45**, 242 (1992).
[3] X. Ling, K. A. Smith, and F. B. Dunning, Phys. Rev. A **47**, R1 (1993); X. Ling, M. T. Frey, K. A. Smith and F. B. Dunning, *ibid.* **48**, 1252 (1993).
[4] F. G. Kellert, K. A. Smith, R. D. Rundel, F. B. Dunning, and R. F. Stebbings, J. Chem. Phys. **72**, 3179 (1980).
[5] C. Higgs, K. A. Smith, G. B. McMillian, F. B. Dunning, and R. F. Stebbings, J. Phys. B. **14**, L285 (1981).
[6] A. Kalamarides, L. N. Goeller, K. A. Smith, F. B. Dunning, M. Kimura, and N. F. Lane, Phys. Rev. A **36**, 3108 (1987).
[7] See, for example, Eq. (9) in O. H. Crawford, J. Chem. Phys. **47**, 1100 (1967).
[8] E. P. Wigner, Phys. Rev. **73**, 1002 (1948).
[9] The Wigner $1/v$ law can be applied only in cases where the interaction potential decreases more rapidly than $1/r^2$.
[10] I. I. Fabrikant, J. Phys. B **16**, 1269 (1983).
[11] I. I. Fabrikant, J. Phys. B **16**, 1253 (1983).
[12] A. S. Wightman, Phys. Rev. **77**, 521 (1950).
[13] W. R. Garrett, Chem. Phys. Lett. **5**, 393 (1970); Phys. Rev. A **3**, 961 (1971); J. Chem. Phys. **73**, 5721 (1980).
[14] C. W. Clark, Phys. Rev. A **20**, 1875 (1979).
[15] L. D. Landau and E. M. Lifshitz, *Quantum Mechanics, Non-Relativistic Theory* (Pergamon, Oxford, 1965), Sec. 143.
[16] I. C. Percival and D. Richards, J. Phys. B **4**, 918 (1971).
[17] W. R. Garrett, J. Chem. Phys. **77**, 3666 (1982).
[18] M. R. C. McDowell and J. P. Coleman, *Introduction to the Theory of Ion-Atom Collisions* (North-Holland, Amsterdam, 1970).
[19] P. C. Engelking and D. R. Herrick, Phys. Rev. A **29**, 2425 (1984).
[20] I. I. Fabrikant, Zh. Eksp. Teor. Fiz. **73**, 1317 (1977) [Sov. Phys. JETP **46**, 693 (1977)]; J. Phys. B **11**, 3621 (1978).
[21] P. C. Engelking, Phys. Rev. **26**, 740 (1982).